Knot spectrum of confined self-avoiding rings

C. Micheletti[1], D. Marenduzzo[2], E. Orlandini[3] and D.W. Sumners[4]

(1) SISSA, CNR-INFM Democritos and Italian Institute of Technology, via Beirut 2-4, Trieste, Italy
(2) School of Physics, University of Edinburgh, Mayfield Road, Edinburgh EH9 3JZ, Scotland
(3) Department of Physics, CNISM and INFN, Universita' di Padova, Via Marzolo 8, Padova, Italy
(4) Department of Mathematics, Florida State University, Tallahasse, FL 32306, USA

Abstract : Advanced stochastic sampling techniques are used to probe the configuration space of self-avoiding flexible rings subject to spatial confinement. The sampled ring conformations are next processed by algorithms that exactly classify knots in rings that are not excessively confined. The physical parameters of the rings, i.e. contour length, bending rigidity and steric hindrance, are properly chosen to mimic the properties of DNA of the P4 bacteriophage, while the radius of the smallest sphere used to confine the model rings is about 2.5 times larger than the P4 capsid radius. By comparing the computed knot spectrum with the P4 one we establish that the consideredmodel correctly predicts an increase of the occurrence of chiral knots with progressive confinement but does not account for the bias of torus versus twist knots observed in P4 experiments.

1 Introduction

Since the early work of Michels and Wiegel [1] the characterization of the knot spectrum in circular chains subject to spatial confinement has represented a challenging and attractive problem [2, 3, 4, 5]. In recent years, the interest in this problem has been stimulated by experiments on the genome of the P4 bacteriophage. In tailless mutants of P4, DNA can circularise inside the viral capsid giving rise to knotted molecules [3, 6]. The analysis of the relative abundance of the simplest DNA knots has revealed a prevalence of chiral versus achiral knots and of torus over twist knots[6].

These observed biases are inconsistent with those found for freely-jointed rings ("phantom" equilateral polygons) subject to high space confinement, which we have previously characterised in ref. [4]. The salient experimental features were instead qualitatively reproduced by spatially-confined freely-jointed rings sampled with a certain bias on the writhe[6].

The results are interesting and stimulate the search for the physical source of the observed bias. As the writhe bias cannot be enforced by local rules governing the chain relaxation inside the capsid we wondered whether, upon addition of physical ingredients in the model such as DNA steric hindrance and bending rigidity, would automatically produce the observed topological bias in confined configurations. This question is motivated by previous observations that imposing suitable spatial confinement conditions on thick polymers is sufficient to promote the selection of ordered and chiral configurations [7, 8, 9, 10, 11, 12].

In the following we shall briefly outline the model, the methodology used to sample the ring configurations and to classify their topology (knotting) and finally discuss the salient features of the knot spectrum. A more detailed account of the study has recently appeared in Ref. [5].

2 Methods

2.1 The model

The P4 DNA is modeled as a flexible ring of 200 cylinders of equal length and diameter. Following the spirit of the simplified DNA models introduced and studies in refs. [13, 14, 15], the statistical weight of a configuration, Γ is given by the Boltzmann weight:

$$e^{-\kappa \sum_i \vec{t}_i \cdot \vec{t}_{i+1} + \gamma \sum'_{i,j} \theta(d^0 - d_{i,j})} \tag{1}$$

where $\vec{t}$ is the ith length-normalised) segment (cylindrical axis) of the ring, κ is a parameter capturing the bending rigidity, d_0 is the diameter of the cylinders, $d_{i,j}$ is the minimum distance of the ith and jth segments (the prime over the summation index is used to indicate that nearest neighbour segments, $i = j \pm 1$, are excluded from the sum) and γ is a very large positive quantity. While the first term is used to model the ring as a closed Kratky-Porod chain (discrete version of the worm-like chain) [16], the second one is used to enforce the finite thickness of the chain by disallowing overlaps of the cylinders constituting the chain. In our study κ and d_0 have been set to values appropriate to model the P4 DNA, which has a contour length of 3.4 μm, $d_0 = 2.5$ nm, and the nominal DNA persistence length (50 nm).

2.2 Biased sampling and multiple Markov chains

A stochastic sampling scheme, based on the Metropolis acceptance/rejection criterion, was used to sample ring configurations according to the canonical weight given by eqn. (1). For entropic reasons, however, most of the sampled configurations will not be compact [17]. To explore efficiently the configuration space of spatially confined rings, an additional pressure-like parameter, $P \geq 0$, was introduced to modify the weight in eqn. (1) into:

$$e^{-\kappa \sum_i \vec{t}_i \cdot \vec{t}_{i+1} + \gamma \sum'_{i,j} \theta(d^0 - d_{i,j})} e^{-PR} \tag{2}$$

where R is the hull radius of the configuration. For computational convenience the latter is defined as the distance from the ring center of mass of the fartherst vertex of the ring. By using increasing values of P the sampling is biased towards more and more compact conformations. The correct canonical weight of the configurations collected through the biased sampling can then be recovered a *posteriori* with standard reweighting techniques [18]. In our study 16 different pressures were used and a Multiple Markov chain scheme [19] was used for the parallel stochastic evolution of the 16 "replicas" of the system.

2.3 Knot simplification and identification

For each pressure, tens of thousands of independent configurations were collected. To identify their knot type, the configurations were first smoothed and shrunk (without altering their topology) so to reduce the average numbers of crossings in a two-dimensional projection. The Dowker code [20] of each simplified configuration was finally used as input for the Knotfind algorithm which, if the projection is not excessively complicated, can identify knots with prime components up to 16 crossings [21]. In Fig. 1a it is shown, as a function of the confining (hull) radius, the fraction of configurations for which we obtain an exact knot classification. It is seen that, as confinement increases, the complexity of the knots projections increases and, consequently, the fraction of configurations for which the knot type can be exactly identified decreases very rapidly.
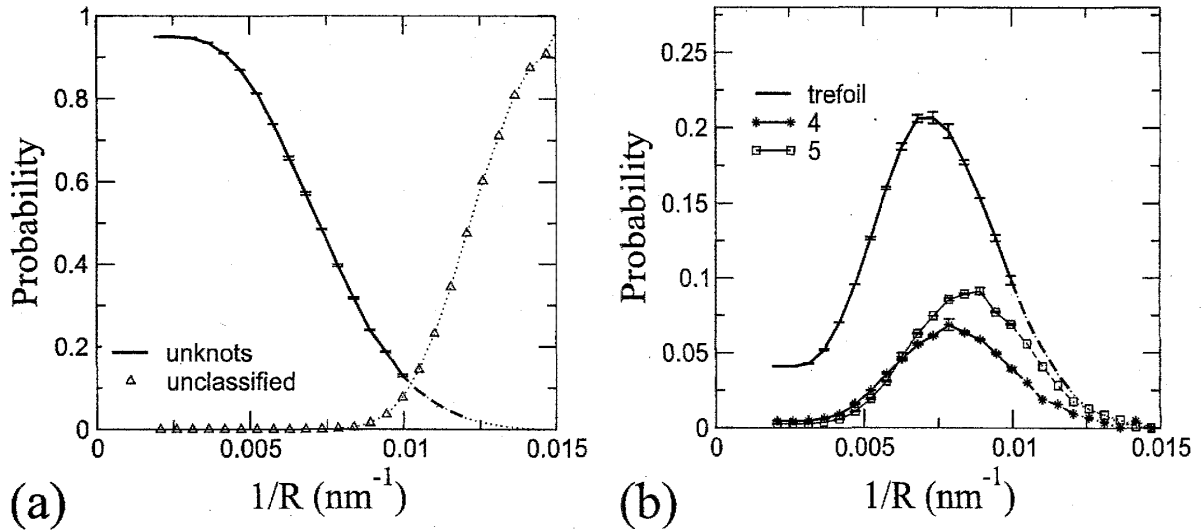
Figure 1: (a) Probability of unknots and of unclassified knots as a function of the inverse radius of the confining sphere, $1/R$, for circular chains of $N = 200$ cylinders. (b) Probability profiles of the simplest knot types. Dashed and dotted lines refer to statistics in which the fraction of unclassified knots is respectively between 10 and 50% and above 50%.

3 Results and conclusions

The occurrence probability of the simplest knot types are shown in Fig. 1b). To remind of the progressive uncertainty on the knot spectrum as confinement is increased, the data are shown with dashed abd dotted lines when the fraction of unclassified knots is respectively between 10 and 50% and above 50%.

We analysed the effect of confinement on the chirality of the knots and the torus versus twist bias. The simplest situation for assessing the effect of chirality bias is to consider the case of knots with 6 minimal crossings. Chiral knots are 6_1, 6_2 and the composite granny knot while achiral ones are 6_3 and the composite square knot. Fig. 2a portrays the trend of the chiral/achiral balance within this group of knots having the same "complexity". Note that, though chiral knots do not significantly outweight achiral ones, there is a growing fraction of chiral knots induced by confinement, which is qualitatively consistent with the observations and conclusions in the P4 experiments.

We next analysed the populations of two types of 5-crossing knots: the 5_1 torus knot and the 5_2 twist knots. This represents the simplest context for examining the effect of confinement on the abundance of torus knots. The probability profiles of the two populations are shown in Fig. 2b. Up to the considered confining radii, the population of the 5_2 twist knots is about twice the one of the 5_1 torus knot. This result is consistent with what observed for confined non-self-avoiding rings [4] but represents an opposite bias to that observed in P4 experiments.

This latest result poses the question of what might be the source for the discrepancy between the experimental data and the computational results. On one hand, it cannot be excluded that the experimentally-observed unbalance between the 5_1 and 5_2 populations sets in at higher levels of confinement. In fact, it should be bourne in mind that the tightest confining radii reached here exceed the P4 capsid radius by a factor of 2.5. On the other hand, it cannot be ruled out that the knot spectrum under high confinement may be affected by physical details not considered here, such as interaction with the capsid interior walls, the shape of the capsid, level of coarse-graining of DNA and its phenomenological elastic parameters etc. Finally, it is possible that out-of-equilibrium effects, reflecting the progressive insertion of DNA inside the capsid by
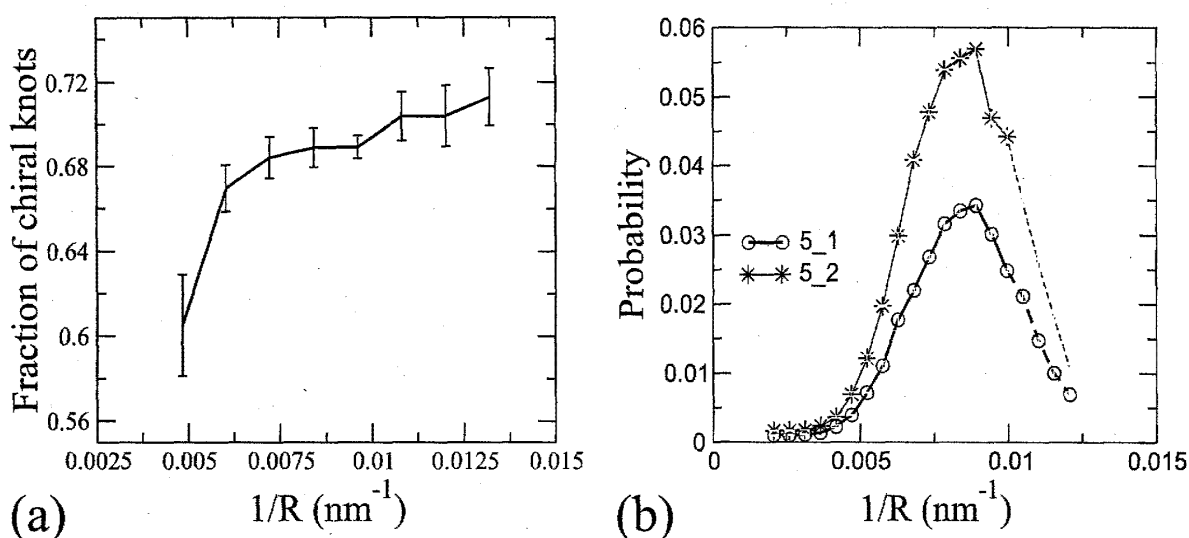
Figure 2: (a) Dependence upon confinement of the fraction of chiral knots (6_1, 6_2 and granny knots) within the knots with 6 minimal crossings (6_1, 6_2, 6_3, granny and square knots). (b) Probability profiles for the 5_1 and 5_2 knots.

the virus portal motor, may not be negligble as one might expect by simple considerations on the diffusion and reptation time of the confined DNA chain. An investigation of these aspects is currently in progress.

Acknowledgments

References

[1] Michels, J. P. J. and F.W. Wiegel. 1986. On the topology of a polymer ring. *Proc. Roy. Soc. A* **403**:269-284.

[2] Mansfield, ML. 1994. Knots in Hamilton cycles. *Macromolecules* 27:5924-5926.

[3] Arsuaga, J., M. Vazquez, S. Trigueros, D.W. Sumners, and J. Roca. 2002. Knotting probability of DNA molecules confined in restricted volumes: DNA knotting in phage capsids. *Proc. Nat. Acad. Sci. USA* 99:5373-5377 (2002).

[4] Micheletti, C., D. Marenduzzo, E. Orlandini and D. W. Sumners. 2006. Knotting of random ring polymers in confined spaces. *J. Chem. Phys.* 124:064903.

[5] Micheletti, C., D. Marenduzzo, E. Orlandini and D.W. Sumners Simulations of knotting in confined circular DNA. *Biophys. J.* 95:3591 (2008)

[6] Arsuaga, J., M. Vazquez, P. McGuirk, S. Trigueros, D. W. Sumners, and J. Roca. DNA knots reveal a chiral organization of DNA in phage capsids. *Proc. Natl. Acad. Sci. USA* 102:9165-9169 (2005).

[7] Maritan, A., C. Micheletti, A. Trovato and J. R. Banavar. 2000. Optimal shapes of compact strings. (2000) *Nature* 406:287-290.

[8] D. Marenduzzo, C. Micheletti, 2003, "Thermodynamics of DNA packaging inside a viral capsid: The role of DNA intrinsic thickness", *J. Mol. Biol.* **330**, 485.

[9] Marenduzzo, D., A. Flammini, A. Trovato, J. R. Banavar and A. Maritan. 2005. Physics of thick polymers. *J. Pol. Sci. B* 43:650-679.

[10] Magee, J. E., V. R. Vasquez, and L. Lue. 2006. Helical structures from an isotropic homopolymer model. *Phys. Rev. Lett.* 96:207802.

[11] Toan, N. M., D. Marenduzzo, P. R. Cook, and C. Micheletti. 2006. Depletion effects and loop formation in self-avoiding polymers. *Phys. Rev. Lett.* 97:178302.

[12] Banavar, J. R., T. X. Hoang, J. H. Maddocks, A. Maritan, C. Poletto, A. Stasiak and A. Trovato. 2007. Structural motifs of biomolecules. *Proc. Natl. Acad. Sci. USA* 104:17283-17286.

[13] Rybenkov, V. V., N. R. Cozzarelli and A. V. Vologodskii. 1993. Probability of DNA knotting and the effective diameter of the DNA double helix. *Proc. Natl. Acad. Sci. USA* 90:5307-5311.

[14] Vologodskii, A. V. and N. R. Cozzarelli. 1995. Modeling of long-range electrostatic interactions in DNA. *Biopolymers* 35:289-296.

[15] Shimamura, M. K., and T. Deguchi. 2000. Characteristic length of random knotting for cylindrical self-avoiding polygons. *Phys. Lett. A*274:184:191.

[16] Marko, J. F. and E.D. Siggia. 1994. Entropic elasticity of lambda-phage DNA. *Science* 265:1599

[17] Millet, K.C. 2001. . An investigation of equilateral knot spaces and ideal physical knot configurations. *Contemp. Math*304, 77 (2002)

[18] Ferrenberg, A. M., and R. H. Swendsen. 1989. Optimized Monte-Carlo data-analysis. *Phys. Rev. Lett.* 63:1195-1198.

[19] Tesi, M. C., E. J. J. Janse van Rensburg, E. Orlandini and S. G. Whittington. 1996. Monte Carlo study of the interacting self-avoiding walk model in three dimensions. *J. Stat. Phys.* 82:155-181.

[20] Dowker, C. H. and M. B. Thistlethwaite. 1983. Classification of knot projections. *Topology Appl.* 16:19-31.

[21] Knotfind is a routine implemented in the KnotScape package created by Jim Hoste and Morwen Thistlethwaite. See for example www.math.utk.edu/ morwen/knotscape.html.